Medicine®

Tissue attenuation imaging and tissue scatter imaging for quantitative ultrasound evaluation of hepatic steatosis

Aladár D. Rónaszéki, MD[a],* , Bettina K. Budai, MD[a], Barbara Csongrády, MD[a], Róbert Stollmayer, MD[a], Krisztina Hagymási, MD, PhD[b], Klára Werling, MD, PhD[b], Tamás Fodor, MD[c], Anikó Folhoffer, MD, PhD[c], Ildikó Kalina, MD, PhD[a], Gabriella Győri, MD[a], Pál Maurovich-Horvat, MD, PhD, DSc[a], Pál N. Kaposi, MD, PhD[a]

Abstract

We aimed to assess the feasibility of ultrasound-based tissue attenuation imaging (TAI) and tissue scatter distribution imaging (TSI) for quantification of liver steatosis in patients with nonalcoholic fatty liver disease (NAFLD). We prospectively enrolled 101 participants with suspected NAFLD. The TAI and TSI measurements of the liver were performed with a Samsung RS85 Prestige ultrasound system. Based on the magnetic resonance imaging proton density fat fraction (MRI-PDFF), patients were divided into ≤5%, 5–10%, and ≥10% of MRI-PDFF groups. We determined the correlation between TAI, TSI, and MRI-PDFF and used multiple linear regression analysis to identify any association with clinical variables. The diagnostic performance of TAI, TSI was determined based on the area under the receiver operating characteristic curve (AUC). The intraclass correlation coefficient (ICC) was calculated to assess interobserver reliability.

Both TAI ($r_s = 0.78$, $P < .001$) and TSI ($r_s = 0.68$, $P < .001$) showed significant correlation with MRI-PDFF. TAI overperformed TSI in the detection of both ≥5% MRI-PDFF (AUC = 0.89 vs 0.87) and ≥10% (AUC = 0.93 vs 0.86). MRI-PDFF proved to be an independent predictor of TAI ($\beta = 1.03$; $P < .001$), while both MRI-PDFF ($\beta = 50.9$; $P < .001$) and liver stiffness ($\beta = -0.86$; $P < .001$) were independent predictors of TSI. Interobserver analysis showed excellent reproducibility of TAI (ICC = 0.95) and moderate reproducibility of TSI (ICC = 0.73).

TAI and TSI could be used successfully to diagnose and estimate the severity of hepatic steatosis in routine clinical practice.

Abbreviations: ALT = alanine transaminase, AST = aspartate aminotransferase, ATI = attenuation imaging, AUC = area under the receiver operating characteristic curve, BMI = body mass index, CAP = controlled attenuation parameter, CI = confidence interval, CSD = liver capsule distance from the skin surface, ICC = intraclass correlation coefficient, LS = liver stiffness, MRI-PDFF = magnetic resonance imaging-based proton density fat fraction measurement, NAFLD = nonalcoholic fatty liver disease, NPV = negative predictive value, PDFF = proton density fat fraction measurement, PPV = positive predictive value, QUS = quantitative ultrasound, ROC = receiver operating characteristic curve, SD = standard deviation, SWE = Shear wave elastography, TAI = tissue attenuation imaging, TE = Echo time, TR = Repetition time, TSI = tissue scatter distribution imaging.

Keywords: liver imaging, nonalcoholic fatty liver disease, quantitative ultrasound imaging, ultrasonography

1. Introduction

Nowadays, the prevalence of nonalcoholic fatty liver disease (NAFLD) is increasing worldwide.[1] Recent studies suggest around 25% prevalence globally.[2,3] If obesity and/or type 2 diabetes are present, the incidental finding of raised liver enzymes in patients with metabolic risk factors should prompt noninvasive screening to predict steatosis, nonalcoholic steatohepatitis (NASH), and fibrosis.[4] NAFLD in some cases leads to NASH, which may lead to fibrosis, cirrhosis, and hepatocellular carcinoma and is a preeminent cause of liver transplantation.[5] Consequently, accurate evaluation of liver fat content is essential in the diagnosis, treatment and follow-up of NAFLD patients.

[a] Department of Radiology, Medical Imaging Centre, Faculty of Medicine, Semmelweis University, Budapest, Hungary, [b] Department of Surgery, Transplantation and Gastroenterology, Faculty of Medicine, Semmelweis University, Budapest, Hungary, and [c] Department of Internal Medicine and Oncology, Faculty of Medicine, Semmelweis University, Budapest, Hungary.

*Correspondence: Aladár D. Rónaszéki, MD, Department of Radiology, Medical Imaging Centre, Faculty of Medicine, Semmelweis University, Korányi Sándor str. 2., H-1082 Budapest, Hungary (e-mail: ronaszeki.aladar_david@med.semmelweis-univ.hu).

For diagnosing and staging liver steatosis, till recently liver biopsy used to be the gold standard method, even though diffuse liver diseases have high spatial heterogeneity leading to sampling error, high inter-reader variability, and invasive side-effects.[6] Therefore, imaging-based, noninvasive methods for fat quantification are highly demanded.[7] Magnetic resonance imaging-based proton density fat fraction (MRI-PDFF) is a robust imaging biomarker; however, it is not routinely performed for clinical screening due to its high cost and limited availability.[8] Recent guidelines suggest ultrasound as the initial diagnostic procedure in patients with NAFLD, as it is a safe, noninvasive, and cost-effective method.[4,9] However, ultrasound-based assessments of liver steatosis are subject to interobserver variability.[10,11] Classical sonographic signs of fatty liver are increased echogenicity relative to the renal cortex, blur of liver parenchyma, poorly visualized portal venous wall and diaphragm.[12] Semiquantitative classifications such as the Hamaguchi index and US-FLI score have poor sensitivity for mild steatosis.[13] Meanwhile, quantitative ultrasound (QUS) techniques determine tissue composition based on acoustic signal analysis, including tissue attenuation imaging (TAI) and tissue scatter distribution imaging (TSI). A significant correlation has already been shown between tissue scattering imaging and MRI-PDFF.[14]

The purpose of our study was to investigate the diagnostic performance of the QUS biomarkers such as TAI and TSI with multiparametric analysis that can be used reliably and reproducibly to determine steatosis in patients with NAFLD using MRI-PDFF as the reference standard.

2. Methods

2.1. Study population and selection criteria

This single-center prospective cohort study was approved by the regional and institutional committee of science and research ethics of our university, and written informed consent was obtained from all participants according to the World Medical Association Declaration of Helsinki, revised in Edinburgh in 2000. We enrolled 110 participants examined for suspected liver steatosis between July 2020 and September 2021. The eligibility criteria to participate in the study included the following: 18 years or older, referral to an imaging study and either ultrasound or MRI for clinically suspected liver steatosis. The participants' demographic data, including the history of alcohol consumption, were collected from a personal survey, the medical history and laboratory tests were collected from electronic medical reports. Participants who reported daily alcohol consumption of ≥20 g (2 drinks) for females or ≥30 g (3 drinks) for males in the last 2 years, as well as patients whose liver iron content was above the normal range (≥2 mg/g) or had a positive genetic test for hereditary hemochromatosis, were excluded from the study (Fig. 1).

The final cohort included 101 subjects (52 females and 49 males), who fulfilled the eligibility criteria, did not meet any of the exclusion criteria and had valid ultrasonography and MRI measurements of hepatic steatosis. The mean age of the participants was 56 years (range 24–78 years). Among the participants, 62 were clinically suspected for NAFLD based on the diagnostic criteria of the European Clinical Practice guidelines.[4] A secondary NAFLD was clinically suspected in 39 patients, as listed in Table 1.

2.2. Quantitative ultrasound-based measurement of hepatic steatosis

All 101 participants were scanned with a Samsung RS85 Prestige ultrasound system (Samsung Medison Co. Ltd., Hongcheon, Korea) using the CA 1-7S convex probe by an expert radiologist with more than 10 years of experience in abdominal ultrasonography. The participants fasted at least 4 hours before the ultrasound scan and were examined in a supine position with the right arm elevated above the head. We performed all QUS measurements in the right liver lobe near the hilum through an intercostal window.[15] To obtain TAI and TSI values, the operator placed a fan-shaped region of interest (ROI) onto the liver parenchyma at least 3 cm below the capsule avoiding large vessels (Fig. 2). The TAI and TSI measurements were repeated 5 times, and the median of the 5 measurements was used for fat quantification. Only TAI values with $R^2 \geq 0.6$ were considered reliable. The TAI was reported in units of dB/cm/MHz, while the TSI was reported in arbitrary units. The distance of the liver capsule from the skin surface (CSD) in mm was also recorded.
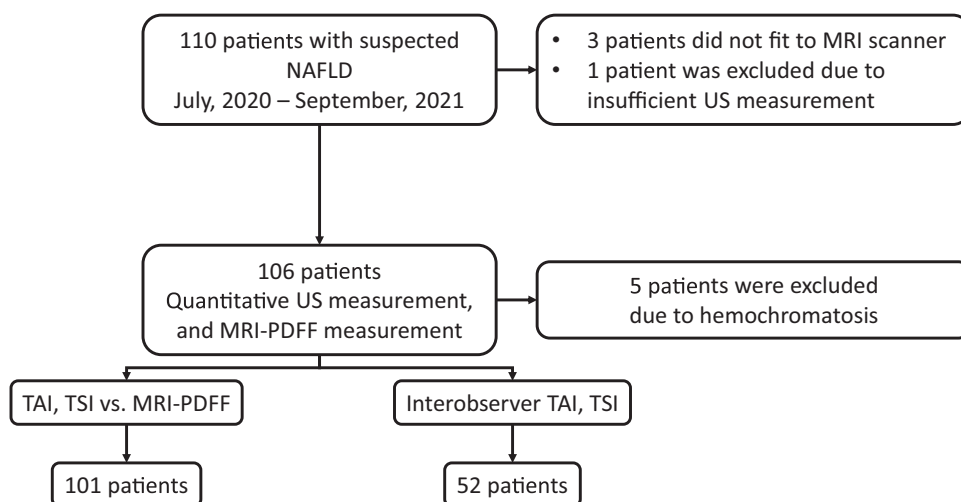

Figure 1. Patient selection and study design. We enrolled 110 participants with suspected NAFLD into this prospective study. One hundred six patients with suspected liver steatosis who fulfilled the inclusion criteria underwent both quantitative ultrasound and MRI-PDFF measurements to determine the liver's fat content. Three morbidly obese patients had been excluded because they did not fit into the MRI scanner, an additional patient was excluded due to failure of the ultrasound measurement, and further 5 patients were excluded due to hemochromatosis, which can interfere with MRI-PDFF. The final patient cohort included 101 NAFLD patients. In 52 cases, 2 examiners independent from each other performed quantitative ultrasound measurements to assess the interobserver reproducibility of TAI and TSI values. MRI-PDFF = magnetic resonance imaging-based proton density fat fraction measurement, NAFLD = nonalcoholic fatty liver disease, TAI = tissue attenuation imaging, TSI = tissue scatter distribution imaging.

Table 1

Demographics of the patient population stratified according to hepatic steatosis.

	All participants and participants without secondary NAFLD etiology			
	All patients	Control (<5% MRI-PDFF)	NAFLD (>5% MRI-PDFF)	P
Total (n)	101	47	54	–
Male (n)	49/101 (48.51%)	27/47 (57.45%)	22/54 (40.74%)	0.094
Age* (yrs)	56.4 ± 12.4	58.1 ± 10.9	54.2 ± 14.0	0.313
Female (n)	52/101 (51.49%)	20/47 (42.55%)	32/54 (59.26%)	–
Age* (yrs)	56.9 ± 12.0	53.7 ± 13.1	59.0 ± 10.9	0.151
P value for age between sex	.693	.33	.223	–
Secondary NAFLD etiology				
Chemotherapy	22/101 (21.78%)	14/47 (29.79%)	8/54 (14.81%)	
Chronic HBV/HCV infection	9/101 (8.91%)	8/47 (17.02%)	1/54 (1.85%)	
AIH	4/101 (3.96%)	2/47 (4.26%)	2/54 (3.70%)	
Wilson disease	4/101 (3.96%)	1/47 (2.13%)	3/54 (5.56%)	
NAFLD				
Total (n)	62	22	40	-
Male (n)	28/62 (45.16%)	10/22 (45.45%)	18/40 (45.00%)	0.973
Age* (yrs)	55.3 ± 14.0	55.1 ± 13.9	55.4 ± 14.5	0.867
Female (n)	34/62 (54.83%)	12/22 (54.55%)	22/40 (55.00%)	–
Age* (yrs)	56.5 ± 12.6	48.3 ± 12.8	60.9 ± 1.2	0.004
P value for age between sex	.552	.487	.276	–

*Reported as mean ± standard deviation.

AIH = autoimmune hepatitis, ALT = alanine aminotransferase, AST = aspartate aminotransferase, BMI = body mass index, HBV = hepatitis B virus, HCV = hepatitis C virus, MRI-PDFF = magnetic resonance imaging-based proton density fat fraction, NAFLD = nonalcoholic fatty liver disease, SD = standard deviation.
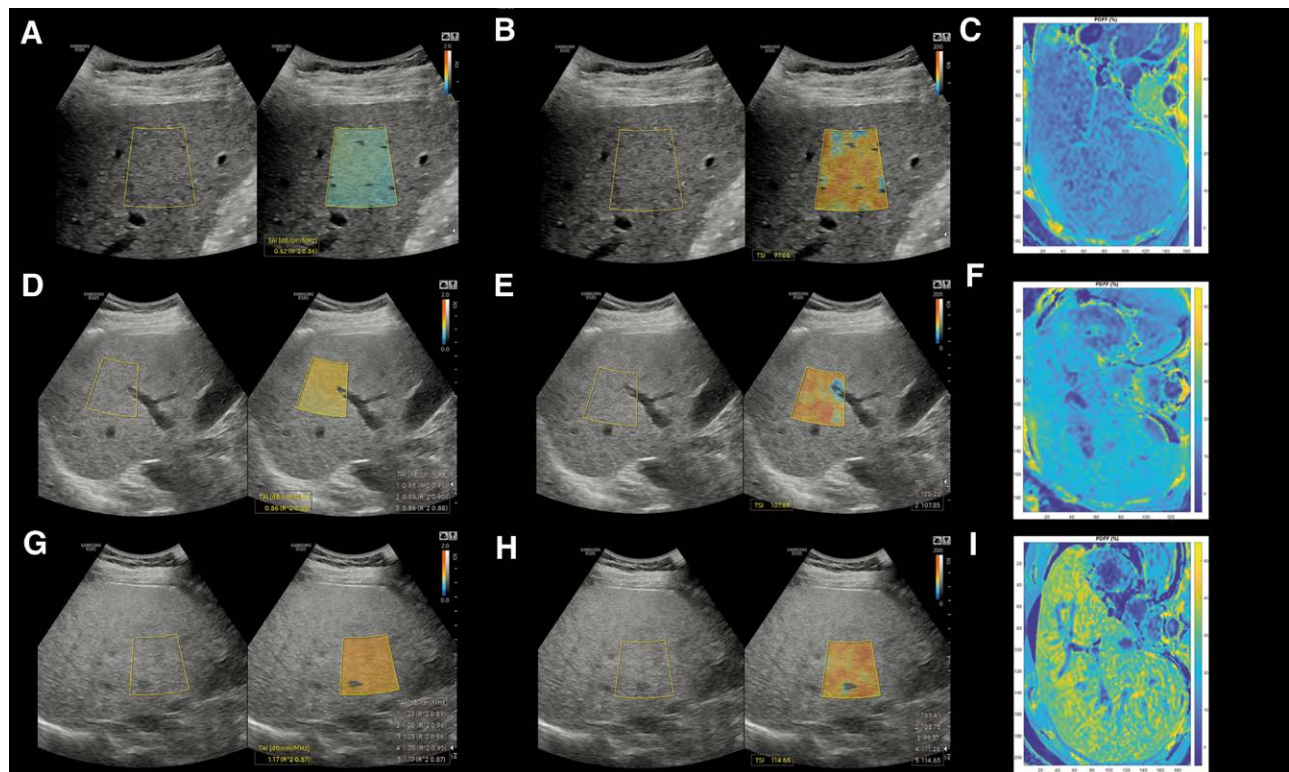

Figure 2. Quantitative ultrasound measurement of the liver fat. Tissue attenuation imaging (A) and tissue scatter distribution imaging (B) of participants with a liver fat content of <5%. For visual reference, colormaps from magnitude-based estimation of MRI-PDFF values were also reconstructed on axial slices where livers with < 5% MRI-PDFF showed blue color indicating no significant steatosis (C). Patients with 5–10% of MRI-PDFF had higher TAI (D) and TSI (E) values compared to patients with no significant hepatic steatosis, while the MRI-PDFF colormap of the liver turned green (F). Finally, patients with ≥ 10% of MRI-PDFF had the highest TAI (G) and TSI values (G), and they had a yellowish color on the MRI-PDFF colormap (I). MRI-PDFF = magnetic resonance imaging-based proton density fat fraction measurement, TAI = tissue attenuation imaging, TSI = tissue scatter distribution imaging.

A second examiner, a trainee with 4 years of experience in abdominal ultrasonography, repeated the QUS measurements in 52 participants on the same day. The examiners were blinded from each other's measurements and the result of MRI-PDFF. In 98 subjects, liver stiffness (LS) was also measured in kPa units using the S-Shearwave Imaging application. For a detailed protocol of shear wave electrography (2D-SWE), we refer to a previous publication.[9]

2.3. Magnetic resonance imaging and measurement of MRI-PDFF

We used the MRQuantif examination protocol and software (https://imagemed.univ-rennes1.fr/en/mrquantif) to measure the magnetic resonance imaging proton density fat fraction (MRI-PDFF) of the livers.[16] In brief, axial images of the liver at the level of the porta hepatis were acquired with a multiecho gradient echo sequence during a single breath-hold of 18 seconds or less. Twelve echos were collected from each slab by changing the echo time (TE) with equally spaced 1.2 ms increments starting from 1.2 ms. Imaging parameters included a flip angle of 20°, a slice thickness of 7 mm, a repetition time (TR) of 120 ms, a field-of-view of 400 × 350 mm, a reconstruction matrix of 128 × 116 pixels, and an interslice gap of 10 mm. A Philips Ingenia 1.5 T MRI scanner (Philips Healthcare, Amsterdam, the Netherlands) and the Q-Body coil were used for all scans. The software calculated the R2* and the MRI-PDFF using an exponential decay model integrating the variation of the signal linked to the 3 main fat peaks determined by Hamilton et al.[17] For visual reference, we used color-coded maps of magnitude-based estimation of MRI-PDFF corrected for multiple fat peaks, field inhomogeneity, and R2* using the MATLAB (The Mathworks, Natick, MA) code (https://github.com/marcsous/pdff) of Bydder et al.[18]

The MRI scan was completed within 1 week of the QUS. A threshold of ≥5% MRI-PDFF was selected to diagnose patients with hepatic steatosis, as recommended by current clinical guidelines.[4] A second threshold at ≥10% MRI-PDFF was used to diagnose fatty liver disease in a more advanced stage.[19,20] We also classified the hepatic steatosis into 4 grades (S0-S3) using the MRI-PDFF cutoff points reported by Park et al.[21]

2.4. Statistical analysis

The normality of the continuous variables was checked by the Shapiro-Wilk test. We used the chi-squared test for estimating the differences between categorical variables, while continuous variables were compared using the Mann-Whitney U test. The differences in clinical parameters between steatosis stages were compared with the Kruskal-Wallis test. During the post hoc Dunn test, the Benjamini-Hochberg method was used for multiple testing corrections. Spearman correlation analysis was performed to assess the correlation between QUS and MRI-PDFF. A receiver operating characteristic (ROC) curve analysis was performed with TAI and TSI to predict the severity of steatosis. The best threshold values were determined based on the closest top-left cutoff point of the ROC curve. We performed a ROC curve power analysis based on the formula described by Obuchowski et al to estimate the smallest sample size that allows for accurate discrimination between categories with a type I error rate of <0.05 and a type II error rate of ≤0.2.[22] Simple and multiple linear regression models were built to identify significant confounding factors of TAI and TSI measurements. We calculated the intraclass correlation coefficient (ICC) using 2-way random effects, absolute agreement, single rater/measurement model to evaluate the inter-rater reproducibility of TAI and TSI.

The statistical analysis was performed with "stats," "dplyr," "regclass," "pROC," "spearmanCI," "dunn.test," and "irr" packages in R v.3.5.3 (www.r-project.org). The threshold of $P < .05$ was used to determine significance in all comparisons.

3. Results

3.1. Detection of liver steatosis in the study population

We prospectively enrolled 101 participants with the suspected fatty liver disease into our study, including 49 (48.5%) males with a mean age of 56 years (range: 36–78 years), as well as 52 (51.5%) females with a mean age of 57 years (range: 24–76 years) (Table 1). The mean body mass index (BMI) (±standard deviation, SD) and the mean LS were 28 kg/m² (±4.37 kg/m²) and 9.1 kPa (±6.0 kPa) in the study population, respectively. The prevalence of significant liver fibrosis (≥F2) among study participants was 34% (34/101).

Among the study participants, 54 (53.5%) had hepatic steatosis (≥5% MRI-PDFF), including 17 (31.5%) patients with ≥5% and <10%, and 37 (68.5%) patients with ≥10% MRI-PDFF. In the cohort, 62 (61.4%) participants were clinically suspected to have NAFLD without secondary etiology, of which 13 (21%) had ≥5% and <10%, and 27 (43.5%) had ≥10% MRI-PDFF (Table 1, Supplemental Digital Content, http://links.lww.com/MD/G977).

We also assigned a steatosis grade (S0-S3) to each participant based on MRI-PDFF. Thus, the study cohort included 38 (37.6%), 35 (34.7%), 6 (5.9%), and 22 (21.8%) participants with S0, S1, S2, and S3 grades hepatic steatosis, respectively.

3.2. Evaluation of the diagnostic performance of TAI for the detection of hepatic steatosis

We found a significant, strong correlation ($r_s = 0.78$, 95% confidence interval [CI = 0.701–0.852], $P < .001$) between TAI and MRI-PDFF values. We also detected a significant positive association (F[1,99] = 101, $P < .001$, R² = 0.51, β = 0.39) between TAI and MRI-PDFF during simple linear regression analysis.

The mean TAI value (0.789 ± 0.08 dB/cm/MHz) of all patients with ≥5% and <10% MRI-PDFF was significantly higher compared with controls without steatosis (0.697 ± 0.10 dB/cm/MHz, Dunn test $P = .009$); also, a significantly higher TAI (0.965 ± 0.14 dB/cm/MHz, $P < .001$) was detected in patients with ≥10% MRI-PDFF compared with other subjects in the hepatic steatosis group (Fig. 3). The mean TAI in the NAFLD cohort also showed significant difference among the groups without steatosis (0.682 ± 0.08 dB/cm/MHz), with ≥5% and <10% MRI-PDFF (0.792 ± 0.09 dB/cm/MHz, $P < .014$) and ≥10% MRI-PDFF (0.95 ± 0.13 dB/cm/MHz, $P < .003$) (Table 1, Supplemental Digital Content, http://links.lww.com/MD/G977).

Including all the 101 participants to the analysis the area under the receiver operating characteristic curve (AUC) of TAI for the detection of ≥5% MRI-PDFF was 0.89 [CI = 0.83–0.95] with power of 1.00 at significance level of $P < .05$ (Fig. 4). The optimal cutoff value at 0.765 dB/cm/MHz had a sensitivity, specificity, negative predictive value (NPV), positive predictive value (PPV) and accuracy of 85%, 79%, 82%, 82%, and 82%, respectively. For the detection of ≥10% MRI-PDFF, the AUC was 0.93 (CI = 0.88–0.98) with power of 1.00 at significance level of $P < .05$; and with a cutoff at 0.845 dB/cm/MHz, the sensitivity, specificity, NPV, PPV, and accuracy were 81%, 89%, 89%, 81%, and 86%, respectively. In the NAFLD cohort, the AUC of TAI for the prediction of ≥5% and ≥10% MRI-PDFF were 0.92 (CI = 0.85–0.98) and 0.93 (CI = 0.87–0.99) both with power of 1.00 at significance level of $P < .05$, respectively. The threshold for diagnosing ≥5% MRI-PDFF in NAFLD was at 0.76 dB/cm/MHz, and for the detection of ≥10% MRI-PDFF at 0.85 dB/cm/MHz, which had a sensitivity, specificity, NPV, PPV, and accuracy of 88%, 86%, 79%, 92%, and 87%, and 78%, 89%, 84%, 84%, and 84%, respectively (Table 2).

A ROC analysis was also performed to determine if TAI measurements can differentiate between steatosis grades. TAI showed excellent performance for both predicting ≥S1 grade (AUC = 0.89, 95% CI = 0.82–0.97) and ≥S2 grade (AUC = 0.85, 95% CI = 0.75–0.95) of hepatic steatosis. The results of this analysis are provided in Table 2 (Supplemental Digital Content, http://links.lww.com/MD/G978), Figure 3 (Supplemental Digital Content, http://links.lww.com/MD/G979), and Figure 4 (Supplemental Digital Content, http://links.lww.com/MD/G980).
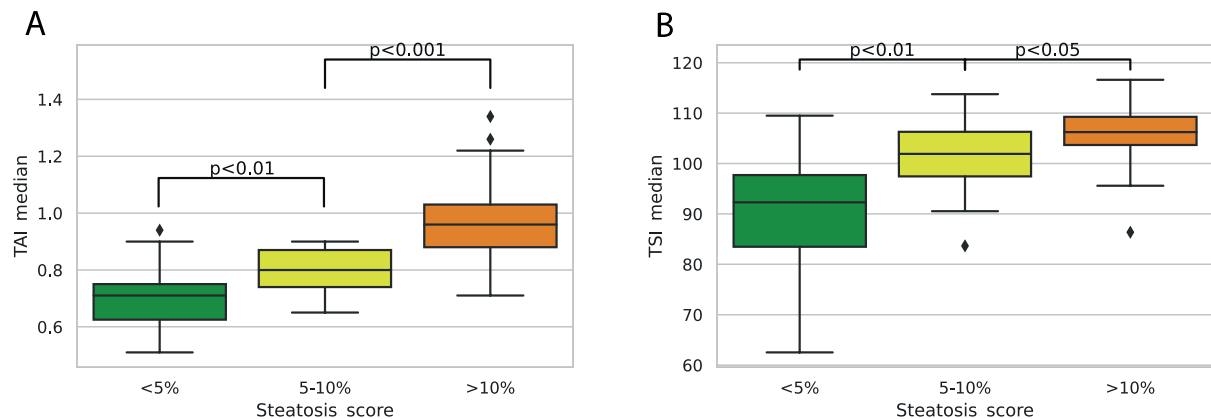
Figure 3. Comparison of quantitative ultrasound metrics between different amounts of hepatic steatosis. Both TAI and TSI showed significant differences between hepatic steatosis of < 5% vs 5–10% vs ≥10% MRI-PDFF. The TSI values showed a greater overlap between the different categories compared to TAI measurements. MRI-PDFF = magnetic resonance imaging-based proton density fat fraction measurement, TAI = tissue attenuation imaging, TSI = tissue scatter distribution imaging.

3.3. Evaluation of the diagnostic performance of TSI for the detection of hepatic steatosis

The correlation between TSI and MRI-PDFF values was strong and significant (r_s = 0.68 (95% CI = 0.578–0.778, $P < .001$)). We also found a significant positive association between TSI and MRI-PDFF ($F[1,99]$ = 40.4, $P < .001$, R^2 = 0.29, β = 0.004) in a simple regression analysis. Consequently, the mean TSI (106.0 ± 5.6) of the group with ≥10% MRI-PDFF was significantly higher than the mean TSI (101.0 ± 7.0, $P < .016$) in hepatic steatosis with ≥5% and <10% MRI-PDFF and the mean TSI (90.7 ± 11.5, $P < .003$) of controls without steatosis (Fig. 3). In NAFLD, the mean TSI was also significantly different among groups without steatosis (91.6 ± 9.7) with ≥5% and <10% MRI-PDFF (102.0 ± 6.2, $P < .007$) and with ≥10% MRI-PDFF (108.0 ± 4.4, $P < .017$) (Table 1, Supplemental Digital Content, http://links.lww.com/MD/G977).

The AUCs of TSI for ≥5% and ≥10% MRI-PDFF were 0.87 (CI = 0.79–0.94) and 0.86 (CI = 0.79–0.93) both with power of 1.00 at significance level of $P < .05$, respectively (Fig. 4). The optimal thresholds to predict ≥5%, and ≥10% MRI-PDFF were at 99.7 and 102.0, which had a sensitivity, specificity, NPV, PPV, and accuracy of 87%, 83%, 85%, 85%, and 85% and 89%, 78%, 93%, 70%, and 82%, respectively. When the ROC analysis was performed on the NAFLD cohort, the AUC of TSI for ≥5% MRI-PDFF was 0.91 (CI = 0.82–0.99), and the AUC for ≥10% MRI-PDFF was 0.88 (CI = 0.79–0.96) both with power of 1.00 at significance level of $P < .05$. The cutoff points were highly similar to those calculated for all participants, including a TSI of 100.6 for ≥5% and a TSI of 103.1 for ≥10% MRI-PDFF resulting in a sensitivity, specificity, NPV, PPV, and accuracy of 88%, 86%, 79%, 92%, and 87% and of 85%, 77%, 87%, 74%, and 81%, respectively (Table 2).

We also performed a ROC analysis for TSI to determine whether it is able to identify patients with at least mild (≥S1 grade) or moderate (≥S2 grade) hepatic steatosis determined by MRI-PDFF. TSI showed comparable results with TAI with AUC of 0.93 (95% CI = 0.86–1.0) for predicting ≥ S1 grade and AUC of 0.813 (95% CI = 0.70–0.92) for predicting ≥ S2 grade in the NAFLD patient cohort. Both TAI and TSI showed very similar classification accuracy in the full cohort including all NAFLD and secondary NAFLD cases, where TAI showed superior performance compared to TSI. The results of this analysis are provided in Table 1 (Supplemental Digital Content, http://links.lww.com/MD/G977), Figure 3 (Supplemental Digital Content, http://links.lww.com/MD/G979), and Figure 4 (Supplemental Digital Content, http://links.lww.com/MD/G980).

3.4. Interobserver reproducibility and reliability of TAI and TSI measurements

In 52 participants, the QUS was repeated by a second examiner on the same day. The correlation between the 2 observers' measurements was excellent for TAI (r_s = 0.94, $P < .001$) and moderate for TSI (r_s = 0.57, $P < .001$). According to the Bland-Altmann plots, the mean of differences between the examiners was 0.01 dB/cm/MHz with TAI and 1.92 with TSI. In the case of both TAI and TSI, most differences (49/52, 94%) fell between the limits of agreement (±1.96 SD), which suggested good reproducibility (Fig. 5). We found excellent interobserver agreement with TAI (ICC = 0.95, 95% CI = 0.91–0.97) and moderate agreement with TSI (ICC = 0.73, 95% CI = 0.56–0.84).

3.5. Analysis of confounding factors of TAI and TSI measurements

Among MRI-PDFF, BMI, CSD, LS, aspartate aminotransferase (AST), and alanine transaminase (ALT), MRI-PDFF was the only independent predictor of TAI in a multivariable regression analysis ($F[3,69]$ = 28.4, $P < .001$, R^2 = 0.53, β = 1.03). Meanwhile, TSI was significantly influenced by both MRI-PDFF (β = 50.9, $P < .001$), and LS (β = −0.86, $P < .001$) in a multivariable model ($F[4,68]$ = 14.4, $P < .001$, R^2 = 0.43) (Table 5, Supplemental Digital Content, http://links.lww.com/MD/G981). We also found significant collinearity between BMI (r_s = 0.49, $P < .001$), CSD (r_s = 0.45, $P < .001$), and MRI-PDFF.

4. Discussion

Recently, multiple noninvasive methods have become available for the quantitative assessment of hepatic steatosis.[23] The main 2 advantages of ultrasound-based hepatic steatosis quantification are the lower cost and the excellent portability of the instrument, which allow for the screening and follow-up of large patient populations. The controlled attenuation parameter (CAP) measurement was the first ultrasound-based technique available for clinical use; however, it requires special instrumentation and has been less accurate for grading steatosis than MRI-PDFF or other ultrasound-based techniques such as attenuation imaging (ATI) and TAI in comparative studies.[21,24] In addition, TAI and TSI can be performed with standard ultrasound scanners; thus, any alterations in liver morphology can be concomitantly evaluated.
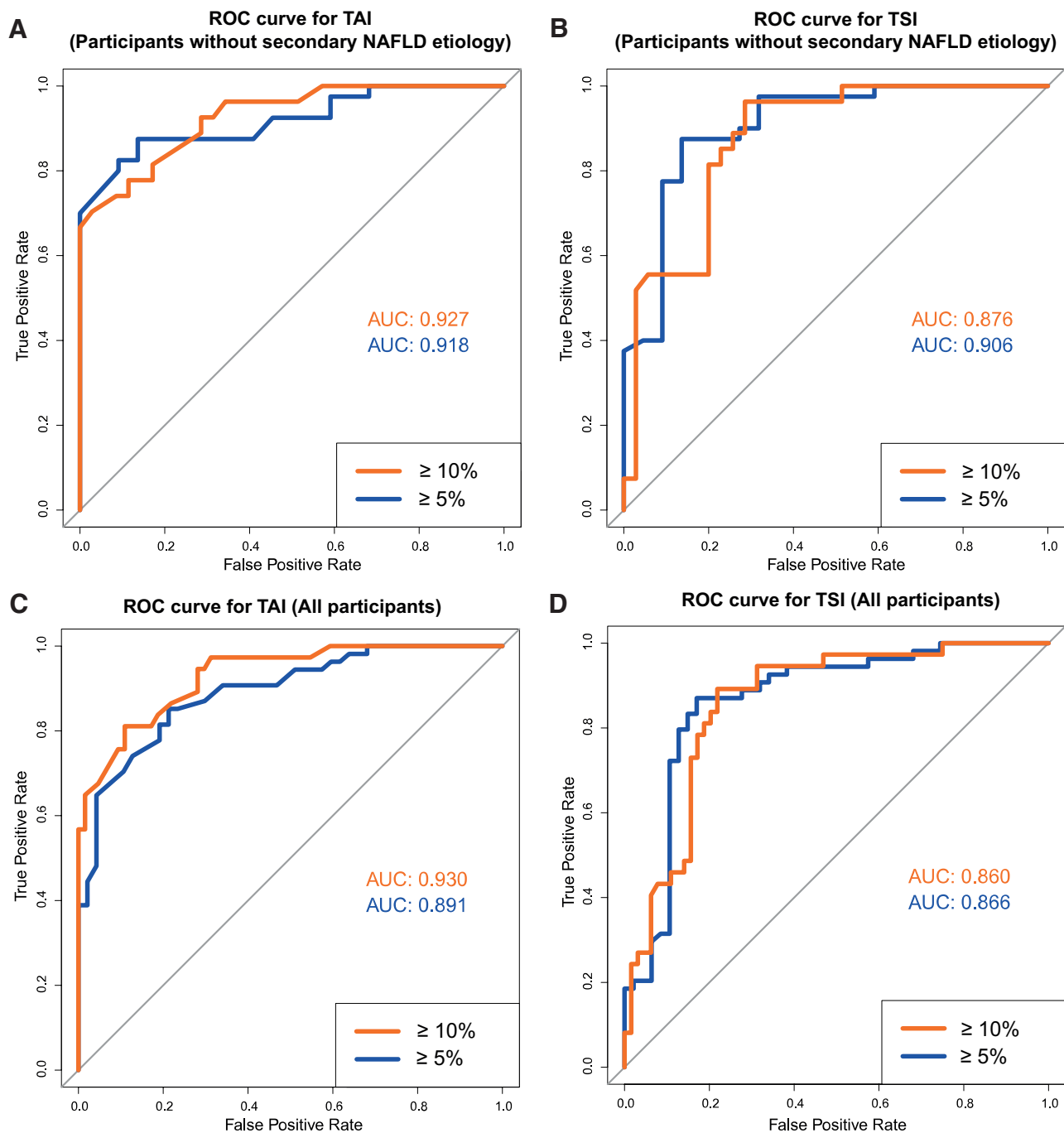
Figure 4. Receiver operating characteristic curve analysis for quantitative ultrasound metrics. According to the receiver operating characteristic curve analysis of NAFLD cases without secondary etiology TAI had excellent AUCs of 0.927 and 0.918 (A), while TSI had very good and excellent AUCs of 0.876 and 0.906 (B), to detect ≥ 5% and ≥ 10% MRI-PDFF, respectively. The TAI (AUC = 0.930 and 0.891) (C) and TSI (AUC = 0.860 and 0.866) (D) had similarly good classification accuracy for ≥ 5% and ≥ 10% MRI-PDFF in all participants. AUC = area under the receiver operating characteristic curve, MRI-PDFF = magnetic resonance imaging-based proton density fat fraction measurement, NAFLD = nonalcoholic fatty liver disease, ROC = receiver operating characteristic curve, TAI = tissue attenuation imaging, TSI = tissue scatter distribution imaging.

Recently, the diagnostic accuracy of TAI was assessed in NAFLD patients in a single-center study by Jeon et al, who reported a moderate correlation between TAI and MRI-PDFF ($R = 0.659$).[20] In our study, TAI showed a strong correlation with MRI-PDFF ($r_s = 0.78$), which was better than the correlation between CAP and MRI-PDFF ($R = 0.53–0.61$) and comparable to the correlation between ATI and MRI-PDFF ($R = 0.81$) reported previously.[24–26] The classification accuracy of TAI was very good for ≥5% (AUC = 0.89) and excellent for ≥10% (AUC = 0.93) MRI-PDFF fat content, and TAI proved to be superior to CAP to diagnose hepatic

steatosis (AUC = 0.69–0.80 and 0.70–0.87, respectively) when our results were compared to prior studies.[19,27]

The correlation between TSI and MRI-PDFF was strong ($r_s = 0.68$), but the coefficient was weaker compared with TAI. Meanwhile, TSI was able to detect ≥5% MRI-PDFF (AUC = 0.87) and ≥10% MRI-PDFF (AUC = 0.86) with very good accuracy, and its ability to diagnose hepatic steatosis was only slightly inferior to TAI. The diagnostic performance of TSI in our study was weaker than the AUC reported for ≥5% and ≥10% MRI-PDFF in a prior study (0.96 and 0.94, respectively),

Table 2

Diagnostic accuracy of quantitative ultrasound metrics for the detection of hepatic steatosis.

NAFLD	AUC*	Threshold	Accuracy	Sensitivity	Specificity	PPV	NPV	Ideal cutoff
TAI								
≥5% MRI-PDFF	0.918 (0.852–0.984)	0.586	0.871	0.875	0.864	0.921	0.792	0.760 dB/cm/MHz
≥10% MRI-PDFF	0.927 (0.86 5–0.989)	0.522	0.839	0.778	0.886	0.84	0.838	0.845 dB/cm/MHz
TSI								
≥5% MRI-PDFF	0.906 (0.824–0.989)	0.681	0.871	0.875	0.864	0.921	0.792	100.64
≥10% MRI-PDFF	0.876 (0.789–0.962)	0.439	0.807	0.852	0.772	0.742	0.871	103.13
NAFLD and secondary NAFLD								
TAI								
≥5% MRI-PDFF	0.891 (0.830–0.952)	0.438	0.822	0.852	0.787	0.821	0.822	0.765 dB/cm/MHz
≥10% MRI-PDFF	0.930 (0.882–0.979)	0.424	0.861	0.811	0.891	0.811	0.891	0.845 dB/cm/MHz
TSI								
≥5% MRI-PDFF	0.866 (0.790–0.943)	0.562	0.852	0.870	0.830	0.854	0.848	99.71
≥10% MRI-PDFF	0.860 (0.787–0.933)	0.393	0.822	0.892	0.781	0.702	0.926	102.045

*Reported as mean and 95% confidence interval.

AUC = area under the receiver operating characteristic curve, MRI = magnetic resonance imaging, NAFLD = nonalcoholic fatty liver disease, NPV = negative predictive value, PDFF = proton density fat fraction, PPV = positive predictive value, SD = standard deviation, TAI = tissue attenuation imaging, TSI = tissue scatter distribution imaging.
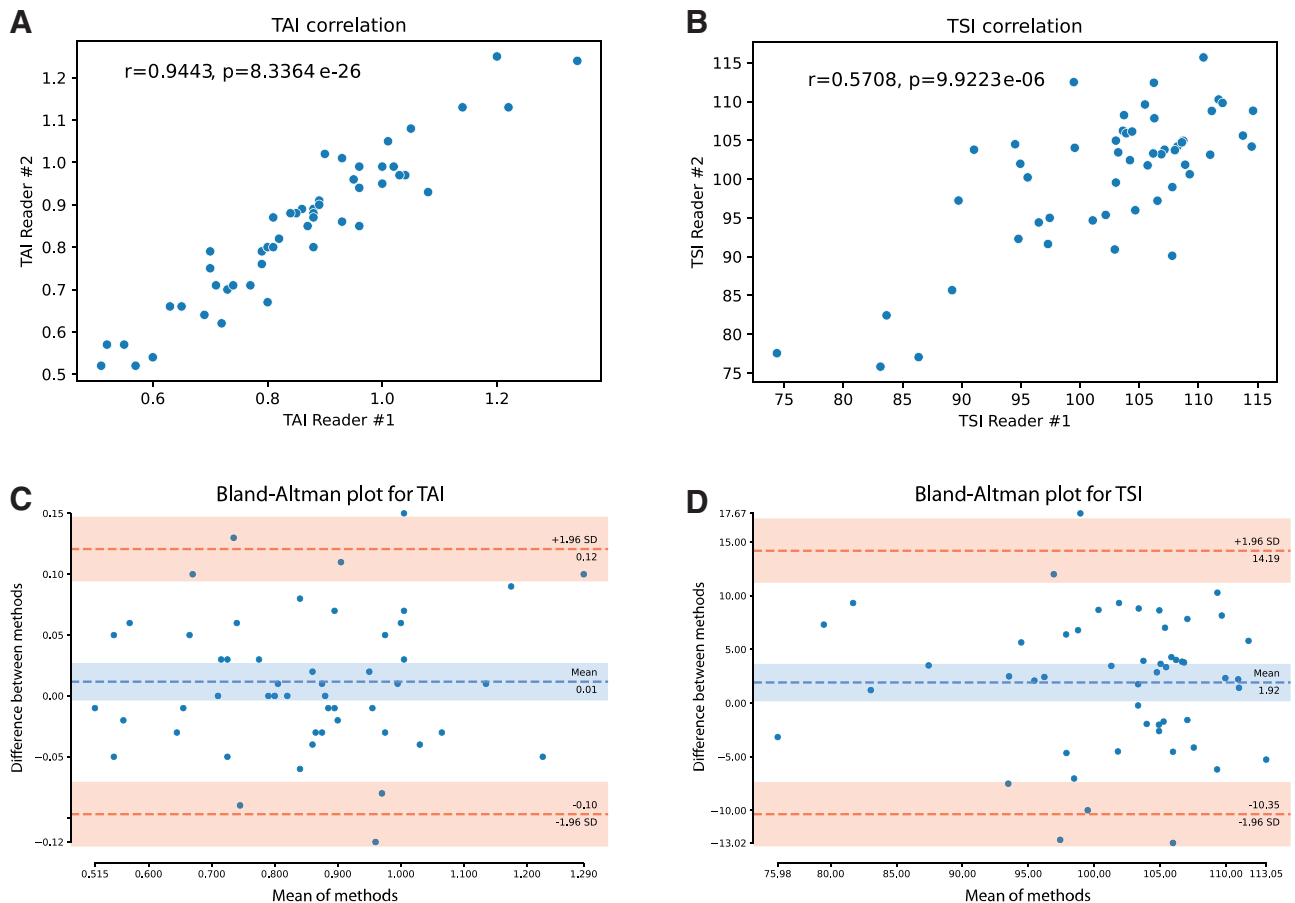

Figure 5. Analysis of interobserver agreement with quantitative ultrasound. The TAI and TSI values measured by the 2 examiners both showed a strong correlation with a Spearman rho of 0.94, $P < .001$ (A) and 0.57, $P < 001$ (B), respectively. The average interobserver difference (dashed blue line) was 0.01 cm/dB/MHz with TAI (C) and 1.92 with TSI (D). Both TAI and TSI showed good reproducibility according to the Bland-Altman plot, where 94% (49/52) of the interobserver differences fell within the 95% confidence interval with limits (dashed red lines) at 1.96 standard deviations. SD = standard deviation, TAI = tissue attenuation imaging, TSI = tissue scatter distribution imaging.

but still exceeded the accuracy of CAP in a similar classification.[19,20] We also found that the interobserver agreement was weaker with TSI than with TAI (ICC = 0.73 vs 0.95) or than the interobserver reliability of TSI in previous studies (ICC = 0.96–0.98), which can be in part attributed to the different levels of experience of the expert and trainee examiners.[20,28]

Our patient cohort consisted of patients who were either diagnosed with NAFLD (61%) on the basis of clinical presentation

or were investigated for secondary NAFLD (39%). The accuracy and the cutoff values of TAI and TSI for the detection of hepatic steatosis were almost identical when the analysis included all participants (TAI = 0.765 dB/cm/MHz, TSI = 99.7) or just NAFLD cases without secondary etiology (TAI = 0.760 dB/cm/MHz, TSI = 100.6). Moreover, the diagnostic thresholds of both TAI and TSI closely matched cutoff values (TAI = 0.884 dB/cm/MHz, TSI = 91.2) reported in a previous study, which investigated solely NAFLD patients.[20] Therefore, we do not consider a significant drawback of our study that it includes NAFLD and secondary NAFLD cases.

We also analyzed the influence of confounding variables on TAI and TSI values. Interestingly, we found a significant negative association between LS measured with 2D-SWE and TSI values. Previously, a similar negative relationship was found between TSI, which represents the Nakagami parameter, and the severity of liver fibrosis detected with transient elastography.[15] Conversely, the Nakagami parameter is derived from the distribution of ultrasound scatter, which follows a Rayleigh distribution in healthy livers and deviates toward a pre-Rayleigh distribution in fibrotic livers.[29]

Our study has several limitations. First, this is a single-center study, which contains a relatively small number of participants. Second, the study cohort was a mix of NAFLD and secondary NAFLD cases, which may hinder the classification of participants, and may cause inaccuracy of the diagnostic thresholds for TAI and TSI. Third, due to selection bias, the prevalence of NAFLD (61%) was significantly higher among participants of the study than in the general population. Fourth, tissue samples were not available for correlation with histopathology.

In conclusion, the liver fat content measured with QUS, using either TAI or TSI, shows a good correlation with MRI-PDFF. Both TAI and TSI are reliable methods for the assessment of hepatic steatosis and can be used to diagnose patients with NAFLD with very good accuracy. TSI may also be helpful in the detection of NAFLD associated liver fibrosis.

Acknowledgments

Author contributions

Aladár D. Rónaszéki - Conceptualization, Data curation, Investigation, Writing – original draft
Bettina K. Budai - Conceptualization, Data curation, Formal analysis, Visualization, Writing – original draft
Barbara Csongrády - Data curation
Róbert Stollmayer - Data curation, Software
Krisztina Hagymási - Conceptualization, Investigation, Validation
Klára Werling - Investigation, Validation
Tamás Fodor - Investigation, Validation
Anikó Folhoffer - Conceptualization, Investigation, Validation
Ildikó Kalina - Resources, Supervision
Gabriella Győri - Investigation, Resources, Supervision
Pál Maurovich-Horvat - Resources, Supervision
Pál N. Kaposi- Project administration, Conceptualization, Methodology, Supervision, Writing – review & editing.

References

[1] Asrani SK, Devarbhavi H, Eaton J, et al. Burden of liver diseases in the world. J Hepatol. 2019;70:151–71.

[2] Mitra S, De A, Chowdhury A. Epidemiology of non-alcoholic and alcoholic fatty liver diseases. Transl Gastroenterol Hepatol. 2020;5:16–16.

[3] Younossi ZM, Koenig AB, Abdelatif D, et al. Global epidemiology of nonalcoholic fatty liver disease-meta-analytic assessment of prevalence, incidence, and outcomes. Hepatology. 2016;64:73–84.

[4] European Association for the Study of the Liver (EASL); European Association for the Study of Diabetes (EASD); European Association for the Study of Obesity (EASO). EASL-EASD-EASO Clinical Practice Guidelines for the management of non-alcoholic fatty liver disease. J Hepatol. 2016;64:1388–402.

[5] Pais R, Barritt AS, Calmus Y, et al. NAFLD and liver transplantation: current burden and expected challenges. J Hepatol. 2016;65:1245–57.

[6] Ratziu V, Charlotte F, Heurtier A, et al. Sampling variability of liver biopsy in nonalcoholic fatty liver disease. Gastroenterology. 2005;128:1898–906.

[7] Ma X, Holalkere NS, Kambadakone RA, et al. Imaging-based quantification of hepatic fat: methods and clinical applications. Radiographics. 2009;29:1253–77.

[8] Reeder SB, Hu HH, Sirlin CB. Proton density fat-fraction: a standardized MR-based biomarker of tissue fat concentration. J Magn Reson Imaging. 2012;36:1011–4.

[9] Folhoffer A, Rónaszéki AD, Budai BK, et al. Follow-up of liver stiffness with shear wave elastography in chronic hepatitis c patients in sustained virological response augments clinical risk assessment. Processes. 2021;9:753.

[10] Kaposi PN, Unger Z, Fejér B, et al. Interobserver agreement and diagnostic accuracy of shearwave elastography for the staging of hepatitis C virus-associated liver fibrosis. J clin ultrasound. 2020;48:67–74.

[11] Strauss S, Gavish E, Gottlieb P, et al. Interobserver and intraobserver variability in the sonographic assessment of fatty liver. AJR Am J Roentgenol. 2007;189:W320–3.

[12] Cengiz M, Sentürk S, Cetin B, et al. Sonographic assessment of fatty liver: intraobserver and interobserver variability. Int J Clin Exp Med. 2014;7:5453–60.

[13] Ibacahe C, Correa-Burrows P, Burrows R, et al. Accuracy of a semi-quantitative ultrasound method to determine liver fat infiltration in early adulthood. Diagnostics (Basel). 2020;10:431.

[14] Lin SC, Heba E, Wolfson T, et al. Noninvasive diagnosis of nonalcoholic fatty liver disease and quantification of liver fat using a new quantitative ultrasound technique. Clin Gastroenterol Hepatol. 2015;13:1337–1345.e1336.

[15] Jeon SK, Joo I, Kim SY, et al. Quantitative ultrasound radiofrequency data analysis for the assessment of hepatic steatosis using the controlled attenuation parameter as a reference standard. Ultrasonography. 2021;40:136–46.

[16] Henninger B, Alustiza J, Garbowski M, et al. Practical guide to quantification of hepatic iron with MRI. Eur Radiol. 2020;30:383–93.

[17] Hamilton G, Yokoo T, Bydder M, et al. In vivo characterization of the liver fat ¹H MR spectrum. NMR Biomed. 2011;24:784–90.

[18] Bydder M, Ghodrati V, Gao Y, et al. Constraints in estimating the proton density fat fraction. Magn Reson Imaging. 2020;66:1–8.

[19] Caussy C, Alquiraish MH, Nguyen P, et al. Optimal threshold of controlled attenuation parameter with MRI-PDFF as the gold standard for the detection of hepatic steatosis. Hepatology. 2018;67:1348–59.

[20] Jeon SK, Lee JM, Joo I, et al. Quantitative ultrasound radiofrequency data analysis for the assessment of hepatic steatosis in nonalcoholic fatty liver disease using magnetic resonance imaging proton density fat fraction as the reference standard. Korean J Radiol. 2021;22:1077–86.

[21] Park CC, Nguyen P, Hernandez C, et al. Magnetic resonance elastography vs transient elastography in detection of fibrosis and noninvasive measurement of steatosis in patients with biopsy-proven nonalcoholic fatty liver disease. Gastroenterology. 2017;152:598–607.e2.

[22] Obuchowski NA, Lieber ML, Wians FH Jr. ROC curves in clinical chemistry: uses, misuses, and possible solutions. Clin Chem. 2004;50:1118–25.

[23] Ferraioli G, Berzigotti A, Barr RG, et al. Quantification of liver fat content with ultrasound: a WFUMB position paper. Ultrasound Med Biol. 2021;47:2803–20.

[24] Ferraioli G, Maiocchi L, Raciti MV, et al. Detection of liver steatosis with a novel ultrasound-based technique: a pilot study using MRI-derived proton density fat fraction as the gold standard. Clin Transl Gastroenterol. 2019;10:e00081e00081.

[25] Beyer C, Hutton C, Andersson A, et al. Comparison between magnetic resonance and ultrasound-derived indicators of hepatic steatosis in a pooled NAFLD cohort. PLoS One. 2021;16:e0249491.

[26] Ferraioli G, Maiocchi L, Savietto G, et al. Performance of the attenuation imaging technology in the detection of liver steatosis. J Ultrasound Med. 2021;40:1325–32.

[27] Shao C, Ye J, Dong Z, et al. Steatosis grading consistency between controlled attenuation parameter and MRI-PDFF in monitoring metabolic associated fatty liver disease. Ther Adv Chronic Dis. 2021;12:20406223211033119.

[28] Jeon SK, Lee JM, Joo I. Clinical feasibility of quantitative ultrasound imaging for suspected hepatic steatosis: intra- and inter-examiner reliability and correlation with controlled attenuation parameter. Ultrasound Med Biol. 2021;47:438–45.

[29] Tsui PH, Ho MC, Tai DI, et al. Acoustic structure quantification by using ultrasound nakagami imaging for assessing liver fibrosis. Sci Rep. 2016;6:33075.